Catalysis Today 65 (2001) 171–177

www.elsevier.com/locate/cattod

Alkane conversion over Pd/SAPO molecular sieves: influence of acidity, metal concentration and structure

M. Höchtl, A. Jentys[1], H. Vinek*

Institute of Physical Chemistry and Theoretical Chemistry, University of Technology, Vienna, Getreidemarkt 9/156, A-1060 Vienna, Austria

Abstract

The activity and selectivity for the isomerization of heptanes over Pd-loaded SAPO molecular sieves with AEL and AFI structure were investigated. By synthesis of the AEL molecular sieves from Al-isopropoxide, the acid site concentration could be controlled by the amount of silicon in the synthesis gel. The resulting concentration of SiAl–OH groups ranged from 0.07 to 0.3 mmol/g, exhibiting the same acid strength, independent from the acid site concentration. Catalysts were impregnated with 0.1–2 wt.% Pd. The activity increased with increasing Pd content up to a Pd to acid site ratio of 0.02–0.03. Above this value, the metal loading did not influence the activity. A further enhancement of the activity was possible by increasing the number of SiAl–OH acid sites. The selectivity to isomerization was constant for the catalysts with an acid site concentration >0.19 mmol/g. The catalysts synthesized from Al-isopropoxide showed a lower activity compared to the catalysts synthesized from aluminum oxide, probably due to diffusional restrictions caused by the formation of polycrystalline agglomerates.

Keywords: Alkane isomerization; SAPO-5; SAPO-11; Acid site concentration; Metal loading

1. Introduction

Hydroisomerization of linear alkanes over bifunctional catalysts based on microporous molecular sieves is a field of widespread interest in crude oil refining. Besides zeolites, crystalline aluminum phosphates can be utilized for hydroconversion reactions [1]. Preferably, mono-dimensional SAPO molecular sieves loaded with a noble metal as hydrogenation promoter were found to be highly selective for the conversion of linear alkanes into monobranched isomers [2,3]. The hydroconversion of *n*-heptane over Pd- or Pt-containing SAPO molecular sieves was extensively reported in the past few years [4–7]. A high selectivity for isomerization to monomethyl-hexanes over SAPO-11 and to mono- and multibranched isomers and a tendency to cracking over SAPO-5 was found [5,8].

The explanation of the preferential formation of terminal monobranched alkanes in 10-membered ring systems like the $AlPO_4$-11 structure, invoked pore mouth catalysis [9,10] restricted transition-state [11–13] or product-shape selectivity [13]. These selectivities are due to the fact that the pore dimensions restrict the formation of bulkier intermediates, therefore terminal branching occurs entirely at the pore mouths, or restrict the motion of bulkier product molecules within the structure. Besides the pore structure, the crystallite size can have a crucial influence

---

* Corresponding author. Tel.: +43-1-588-0115650; fax: +43-1-588-0115699.
E-mail address: vinek@tuwien.ac.at (H. Vinek).

[1] Present address: Institute of Technical Chemistry II, Technical University of Munich, Lichtenbergstr. 4, D-85747 Garching, Germany.

PII: S0920-5861(00)00581-2

on the catalytic performance of hydroisomerization catalysts [14]. Small changes in either the pore diameter or the molecular size can change the diffusivity of alkanes by orders of magnitude [15].

The hydroconversion of *n*-alkanes over bifunctional catalysts is supposed to proceed via a bifunctional mechanism that was suggested by Weisz and Swegler [16]. In the first step the *n*-alkane is dehydrogenated on the metal site. The alkene is isomerized and can undergo β-scission on the acid site. The reaction selectivity towards hydroisomerization or hydrocracking is determined by the lifetime of the intermediate carbenium ions, which depend on the structure of these carbonium ions, the diffusion coefficients of the reactants and products, the temperature, the acid strength of the molecular sieve and the hydrogenation activity of the metal component.

In SAPO molecular sieves, various types of hydroxyl groups like terminal Al–OH, Si–OH and P–OH and bridged SiAl–OH are present [3]. Bridged acid sites are, in contrast to terminal hydroxyl groups, active for hydrocarbon skeletal rearrangement [17].

The main objective of this work was to determine the activity and selectivity in hydroisomerization of *n*-heptane and heptane isomers over two series of Pd/SAPO-11, synthesized by different methods, and Pd/SAPO-5. The influence of the concentration of acid and metal sites on the reaction mechanism was investigated.

2. Experimental

2.1. Synthesis

SAPO-11 and SAPO-5 molecular sieves were prepared by hydrothermal synthesis, as described in the patent literature [18,19]. Two series of SAPO-11 were synthesized, series A with pseudoboehmite (Condea Pural NG) and series B with aluminum isopropoxide (Aldrich) as aluminum sources. In Table 1, the product compositions in mole percent of the oxides are given. $AlPO_4$-11 was prepared according to a method by Tapp et al. [20]. The template was triethylamine for AFI structure and di-*n*-propylamine (Fluka) for AEL structure materials.

After washing with distilled water and drying at 110°C, the samples were calcined in air at 600°C until the template was completely removed. The chemical composition of the calcined products was determined by EDX.

Table 1
Chemical and physical properties of SAPO-11 and SAPO-5 samples

	Product (mol%)			BET (m^2/g)	SiAl–OH (mmol/g)
	Al	P	Si		
SAPO-11 (series A) pseudoboehmite					
A1	61.0	36.6	2.4	174	0.19
A2	52.2	44.9	2.9	184	0.23
A3	51.2	45.6	3.2	180	0.29
A4	48.6	48.7	2.7	182	0.30
SAPO-11 (series B) Al-isopropoxide					
B1	49.7	49.7	0.6	214	0.07
B2	49.7	49.4	0.9	154	0.09
B3	48.4	49.4	2.2	200	0.14
B4	48.8	49.1	2.1	202	0.24
B5	49.5	47.8	2.7	185	0.27
SAPO-5	45.6	45.9	8.5	339	0.24

Catalysts containing 0.1–2 wt.% palladium ($Pd(NH_3)_4Cl_2\cdot H_2O$) were prepared by the incipient wetness method. After impregnation, the samples were slowly heated to 70°C and finally dried at 110°C. The metal precursor was decomposed in flowing oxygen at 450°C and subsequently the metal was reduced in hydrogen at the same temperature.

Hybrid catalysts were prepared by mechanically mixing Pd-impregnated SiO_2 and calcined SAPO-11/A4. This catalyst was used in the manually mixed form or compressed with 1 t/cm^2 pressure and subsequently crushed in a mortar.

Temperature programmed desorption (TPD) of ammonia and pyridine was used to qualitatively and quantitatively characterize the acidity of the molecular sieves.

The infrared (IR) spectra were recorded on a Bruker IFS28 Fourier transform IR-spectrometer with a resolution of 4 cm^{-1} equipped with an MCT-detector. Samples of 8–15 mg were pressed into self-supporting disks with a diameter of 2 cm. The adsorption of benzene was carried out in a pressure range of 10^{-4}–1 mbar at 40 and 150°C, respectively. Spectra were recorded every 30 s to observe the approach to the adsorption equilibrium.

The Pd dispersion was determined from a hydrogen adsorption isotherm measured in a volumetric adsorption apparatus following a method suggested by Benson et al. [21].

The morphology and the particle size of the materials were estimated from scanning electron microscope (SEM) measurements.

The hydroconversion experiments were carried out in a quartz glass downstream plug flow reactor with 4 mm inner diameter. The reactor was filled with 5–30 mg catalysts, diluted with the equal amount of quartz sand to stabilize the flow conditions. Prior to the reaction, the samples were activated in oxygen at 450°C for 1 h and reduced in hydrogen for another hour at the same temperature. Heptane (25 mbar) was added via a saturator to the hydrogen reaction gas stream. The reaction conditions were 3 bar total pressure, $H_2/C7 = 120$ and temperature 300°C. The reaction products were analyzed with an HP 5980 II gas chromatograph equipped with a flame ionization detector.

3. Results and discussion

Using Al-isopropoxide (series B), the silicon content of the SAPO-11 depended on the amount of SiO_2 used in the synthesis gel (see Fig. 1A). Furthermore, the number of bridged SiAl–OH groups that can act as Brønsted acid sites, correlated with the Si incorporated in the SAPO lattice. However, the number of bridged acid sites was below the theoretical value, when each Si atom generated a negative charge on the SAPO lattice (Fig. 1B). HSAPO-5 molecular sieves with various Si concentrations were synthesized by Masukawa et al. [22]. They found an agreement of the acid site concentration and the theoretical value calculated from the Si atomic ratio below 0.02, assuming that every Si atom leads to the formation of one acid site (SM2). In contrast to these results, even at low Si contents a part of the silicon was incorporated into the framework of SAPO-11 via SM3 [23]. The observed concentration of strong acid sites was therefore lower than the calculated value for all samples (Fig. 1B).

For the composition of the series A materials, no correspondence with the gel composition was observed. However, SAPO molecular sieves with different densities of bridged SiAl–OH Brønsted acid sites were obtained (Table 1).

For the SAPO-11 (series A) an inhomogeneous particle size distribution was found (Fig. 2a). The crystals were in the shape of prisms and plates with a diameter between 1 and 5 μm, but did not exhibit larger agglomerates or oligocrystalline intergrowth. In contrast, SAPO-11 (series B) exhibited polycrystalline spheres with a diameter of 10–20 μm which consisted of prisms and needles with a length of 2–5 μm (Fig. 2b).

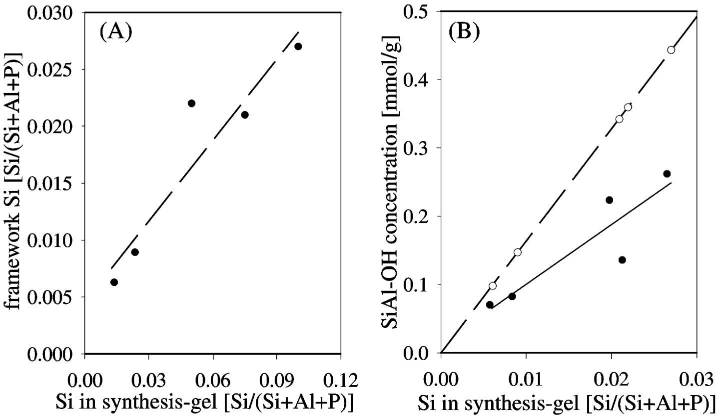

Fig. 1. (A) Dependence of the Si content of the calcined SAPO-11 (EDX) on the Si molar ratio in the synthesis gel (series B). (B) Incorporated Si versus number of strong acid sites (bridged SiAl–OH groups); the dashed line indicates the value of acid sites calculated from the Si content.

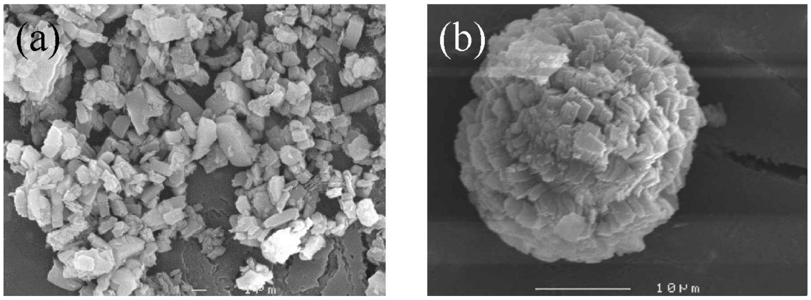

Fig. 2. Scanning electron micrographs: (a) SAPO-11 (series A); (b) SAPO-11 (series B).

3.1. Acid and metal sites on SAPO-11 and SAPO-5

The desorption profiles of ammonia on SAPO molecular sieves showed two maxima. The first maximum around 110°C was assigned to weakly bound ammonia and the second maximum at 200°C for SAPO-5 and 225°C for SAPO-11 was due to ammonia desorbed from bridged hydroxyl groups [24]. The third peak around 160°C was added to the fit in order to take account of the ammonia desorption from terminal P–OH groups, as observed by NH_3-TPD from $AlPO_4$-11 [25]. The number of acid sites determined by pyridine and NH_3-TPD was essentially the same. Furthermore, no change of the acid site density was observed after impregnation with Pd.

The IR-spectra of SAPO-5 and SAPO-11 showed five bands in the OH stretching vibration domain: Al–OH bands at 3800 cm^{-1}, Si–OH bands at 3745 cm^{-1}, P–OH bands at 3676 cm^{-1}, bridged SiAl–OH bands (Brønsted acid sites) at 3628 cm^{-1}, and a broad band at 3530 cm^{-1}, which can be assigned to bridged OH groups interacting with the oxygen atoms of the framework [3].

The interaction of benzene as weak base with Brønsted acid sites leads to a shift of the OH frequency to lower wavenumbers [26]. The extend of the shift depends on the strength of the interaction and thus corresponds to the acid strength of the hydroxyl groups [27]. The red shift of the OH stretching vibrations was about 310 cm^{-1}, independent of the acid site concentration, on the SAPO-11 series B (see Fig. 3) as well as on series A molecular sieves. The shift of the bridged OH groups of SAPO-5 was 280 cm^{-1}, and that of the P–OH groups about 220 cm^{-1}.

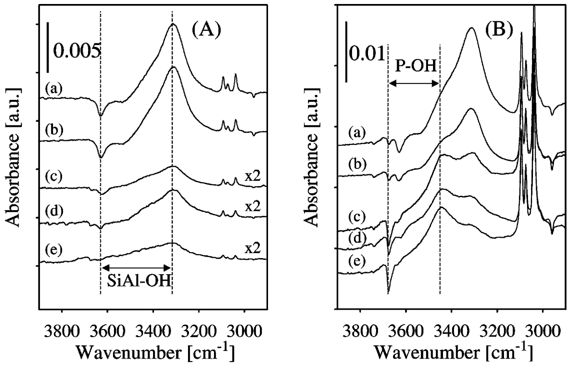

Fig. 3. IR-difference spectra of SAPO-11, series B after adsorption of 10^{-3} mbar (A) and 1 mbar (B) benzene: (a) SAPO-11/B5, (b) SAPO-11/B4, (c) SAPO-11/B3, (d) SAPO-11/B2, (e) SAPO-11/B1.

The dispersion of palladium on the different SAPO-11 samples and on SAPO-5 at a metal loading of 1% or higher was always below 10%, while for the samples with 0.1 wt.% Pd on SAPO-11, the dispersion was between 30 and 40% (Fig. 4). For dispersion below 10%, the metal particles must be mainly located on the outer surface of the aluminum phosphate grains. Calculating the metal/acid site ratio for the different SAPO-11 samples, it was found that above a ratio of 0.02–0.03, the metal concentration had no influence on the *n*-heptane conversion rate. Therefore, a metal loading of 1 wt.% Pd is necessary to provide sufficient metal sites for the rapid paraffin dehydrogenation and the hydrogenation of the products.

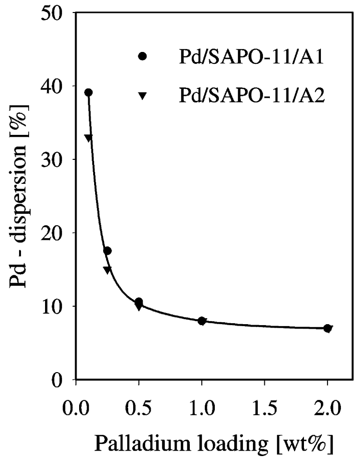

Fig. 4. Dependence of the Pd-dispersion on the Pd-loading.

3.2. Heptane conversion

In Fig. 5, the activity of the *n*-heptane and 2,3-dimethyl-pentane conversion at 300°C as a function of the number of Brønsted acid sites of the investigated Pd/SAPO-11 samples are shown. The conversion rate over Pd-loaded $AlPO_4$-11, a catalyst containing no strong acid sites, was inserted. The total rate of the heptane conversion increased slightly below 0.1 mmol/g acid, whereas in the range between 0.1 and 0.3 mmol/g, a steep increase was observed.

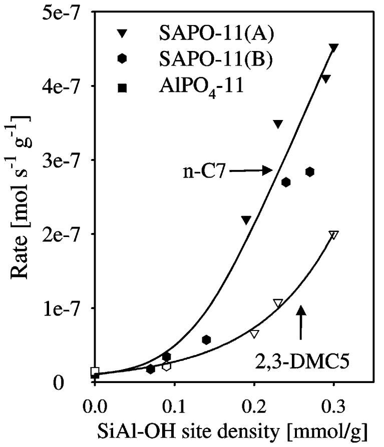

Fig. 5. Dependence of the *n*-C7 and the 2,3-DMC5 conversion on the acid site density.

The isomerization selectivity increased with increasing acid site density and reached 95% for samples with an acid site density above 0.15 mmol/g. Below 0.15 mmol/g acid site density the isomerization selectivity was between 700 and 90%. Only small amounts of 2,3- and 2,4-dimethyl-pentane (∼1%) were detected over the Pd/SAPO-11 samples. The absence of 2,2- and 3,3-dimethyl-pentane in the product distribution confirms that those molecules are excluded from the pores of SAPO-11. Over SAPO-5 additionally these isomers and 3-ethylpentane were found. The activity of 2- and 3-methylhexane was higher than that of *n*-heptane over both molecular sieves. The main reaction path of the monobranched isomers (Fig. 6) was isomerization via a methyl shift. Furthermore, *n*-heptane over SAPO-11 and dibranched isomers over SAPO-5 were found as products. Even for the conversion of 2,3-dimethyl-pentane, a correlation between the activity and the number of Brønsted acid sites was confirmed for SAPO-11. But the steric constraints of the pores led to a much lower activity for the 2,3-dimethyl-pentane conversion compared to SAPO-5. However, the dependence of the activity on the number of acid sites and the high selectivity to *n*-heptane suggested that the reaction occurred inside the pores of SAPO-11 (Fig. 5). The results presented are in agreement with Maesen et al. [28], who found that mono methyl-alkanes and dimethyl-alkanes with methyl groups in vicinal positions are able to enter the pores of AEL molecular sieves.

The non-linear dependency of the activity on the number of SiAl–OH sites could be explained by the different substitution of Si in the $AlPO_4$ molecular sieves. Masukawa et al. [22,29] investigated *o*-xylene isomerization over a series of HSAPO-5 molecular sieves. They found a low activity of their catalysts with a concentration of strong acid sites less than 0.2 mmol/g and a steep increase for catalysts with a higher number of acid sites. They concluded that at low Si contents, Si is substituted for single P atoms by SM2. These Si/Al–OH groups exhibited a lower acid strength and activity than SiAl–OH groups in $SiAlO_4$-domains, formed at higher Si concentrations. Although it was shown by benzene adsorption that the acid strength of all SAPO molecular sieves is approximately in the same range, there could be minor differences that cannot be distinguished by the method applied. However, it is also possible that a part of

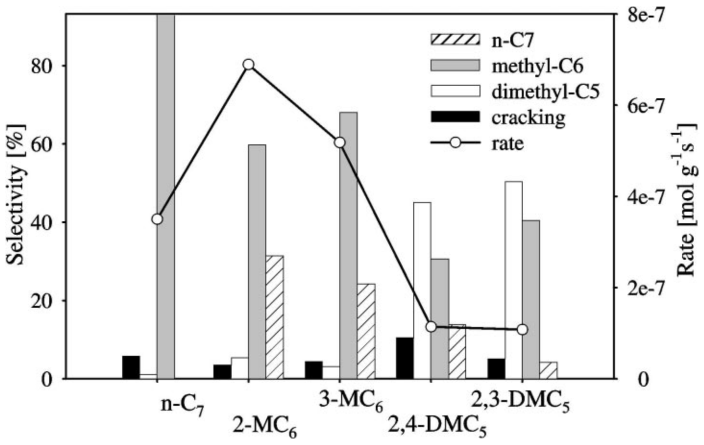

Fig. 6. Rate and selectivity of the reaction of different heptane isomers over 1 wt.% Pd/SAPO-11.

the acid sites in the low silicon samples (SAPO-11/B1–B3) is not accessible for molecules larger than ammonia. TPD of pyridine and adsorption of benzene and hydrocarbons followed by IR spectroscopy on these materials show an incomplete coverage of the SiAl–OH groups. In contrast, on SAPOs with high silica content, a complete accessibility of the SiAl–OH groups for the later probe molecules was detected.

To investigate the influence of the distance between metal and acid sites, Pd-impregnated silica was mechanically mixed with SAPO-11/A2 and used as parent mixture and in compressed form. In Fig. 7, those catalysts (B and C) are compared to Pd impregnated on SAPO-11 (A). The hybrid catalyst closely resembled the activity of the impregnated Pd/SAPO-11 catalyst, while the isomerization selectivity was slightly lower. When the acid and metal sites were complete separated by dividing the catalyst into two layers (D) the synergetic effects of the bifunctional behavior disappeared. The product distribution was similar to that over Pd/SiO$_2$ (E). Additionally, the results for the *n*-heptane conversion over Pd/AlPO$_4$-11(F) are given. Assuming that the first step of the hydroisomerization reaction is the dehydrogenation of the linear alkanes, these experiments verified that unsaturated intermediates exist, which are able to migrate between the metal and the acid sites, where subsequently the isomerization reactions occur.

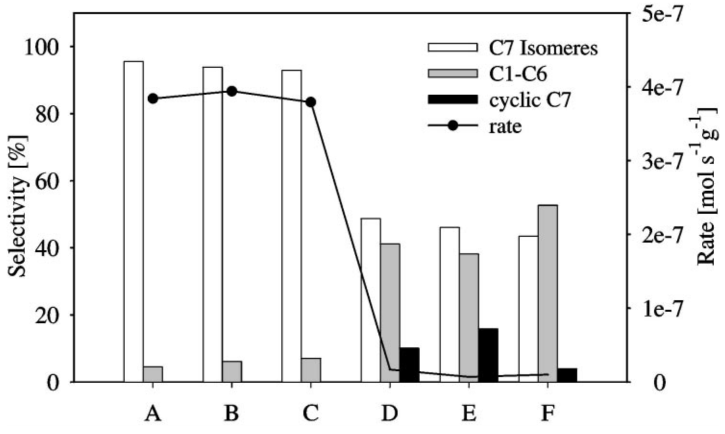

Fig. 7. Selectivity and activity of differently prepared 1 wt.% Pd/SAPO-11.

4. Conclusions

- The Si molar fraction of the SAPO-11 molecular sieves can be controlled by the silicon content of the synthesis gel, provided that aluminum isopropoxide is used as aluminum source. In this case, the SiAl–OH concentration is proportional to the Si concentration.
- Pd-loaded SAPO-11 are highly selective catalysts for the hydroisomerization of normal alkanes. The activity of the catalysts depends strongly on the acidity of the molecular sieves.
- The acid strength of bridged SiAl–OH groups does not change with the acid site concentration.
- The ideal Pd to SiAl–OH ratio was 0.02–0.03. A further enhancement of either the selectivity or the activity by increasing the metal content is not possible.
- SAPO-11–Pd/SiO_2 hybrid catalysts exhibit almost the same activity and selectivity as the impregnated SAPO-11 materials.
- The synergism between metal and acid sites of a bifunctional catalyst is independent of their distance, unless the supported metal is completely separated from the acidic material.
- Spillover hydrogen may be the reason for the acceleration of the isomerization in the presence of a hydrogen activating metal. However, the activated hydrogen must migrate on the solid surface of the support or the molecular sieve, since no gas phase transport was observed.
- Pd/SAPO-11 exhibits a higher activity for the *n*-heptane isomerization than Pd/SAPO-5. Due to the larger pores of SAPO-5, the branched C7-isomers react faster.

Acknowledgements

The work was supported by the “Fonds zur Förderung der Wissenschaftlichen Forschung” (Project P11479).

References

[1] S.J. Miller, Stud. Surf. Sci. Catal. 84 (1994) 2319.
[2] J.M. Campelo, F. Lafont, J.M. Marinas, J. Chem. Soc., Faraday Trans. 91 (1995) 1551.
[3] P. Mériaudeau, V.A. Tuan, V.T. Nghiem, S.Y. Lai, L.N. Hung, C. Naccache, J. Catal. 169 (1997) 55.
[4] J.M. Campelo, F. Lafont, J.M. Marinas, J. Catal. 156 (1995) 11.
[5] B. Parlitz, E. Schreier, H.L. Zubowa, R. Eckelt, E. Lieske, G. Lischke, R. Fricke, J. Catal. 155 (1995) 1.
[6] M.A. Chaar, J.B. Butt, Appl. Catal. A 114 (1994) 287.
[7] A.K. Sinha, S. Sivasanker, Catal. Today 49 (1999) 293.
[8] M. Höchtl, A. Jentys, H. Vinek, J. Catal. 190 (2000) 419.
[9] W. Souverijns, J.A. Martens, G.F. Froment, P.A. Jacobs, J. Catal. 174 (1988) 177.
[10] J.A. Martens, W. Souverijns, W. Verrelst, R. Parton, G.F. Froment, P.A. Jacobs, Angew. Chem. Int. Engl. 34 (1995) 2528.
[11] S.J. Miller, Microporous Mater. 2 (1994) 439.
[12] P.A. Jacobs, J.A. Martens, J. Weitkamp, H.K. Beyer, Faraday Discuss. Chem. Soc. 72 (1982) 353.
[13] J.A. Martens, P.A. Jacobs, Zeolites 6 (1986) 334.
[14] P. Mériaudeau, V.A. Tuan, F. Lefebvre, V.T. Nghiem, C. Naccache, Micropor. Mesopor. Mater. 22 (1998) 435.
[15] N.Y. Chen, T.F. Degnan, C.M. Smith, Molecular Transport and Reaction in Zeolites, VCH, New York, 1994, p. 131 ff.
[16] P.B. Weisz, E.W. Swegler, Science 126 (1957) 31.
[17] J.A. Martens, M. Tielen, P.A. Jacobs, Stud. Surf. Sci. Catal. 46 (1989) 49.
[18] B.M. Lok, C.A. Messina, R.L. Patton, R.T. Gajek, T.R. Cannan, E.M. Flanigen, US Patent No. 4 440 871 (1984).
[19] E.M. Flanigen, B.M. Lok, R.L. Patton, S.T. Wilson, in: Y. Murakami, A. Iijima, J.W. Ward (Eds.), New Developments in Zeolite Science and Technology, Surface Science and Catalysis, Vol. 28, Elsevier, Amsterdam, 1986, p. 103.
[20] N.J. Tapp, N.B. Milestone, D.M. Bibby, Zeolites 8 (1988) 183.
[21] J.E. Benson, H.S. Hwang, M. Boudart, J. Catal. 30 (1973) 146.
[22] T. Masukawa, T. Komatsu, T. Yashima, Zeolites 18 (1997) 10.
[23] M. Mertens, J.A. Martens, P.J. Grobet, P.A. Jacobs, Guidelines for Mastering the Properties of Molecular Sieves, Plenum Press, New York, 1990, p. 1.
[24] U. Lohse, B. Parlitz, E. Löffler, E. Schreier, B. Altrichter, K. Jancke, F. Vogt, J. Chem. Soc., Faraday Trans. 91 (1995) 1155.
[25] M. Höchtl, A. Jentys, H. Vinek, Micropor. Mesopor. Mater. 31 (1999) 271.
[26] A. Jentys, J.A. Lercher, in: H.G. Karge, J. Weitkamp (Eds.), Zeolites as Catalysts, Sorbents and Detergent Builders, Studies on Surface Science and Catalysis, Vol. 46, Elsevier, Amsterdam, 1989, p. 585.
[27] M.L. Hair, Infrared Spectroscopy in Surface Chemistry, Marcel Dekker, New York, 1967, p. 132.
[28] Th.L.M. Maesen, M. Schenk, T.J.H. Vlugt, J.P. de Jonge, B. Smit, J. Catal. 188 (1999) 403.
[29] T. Masukawa, T. Komatsu, T. Yashima, Zeolites 19 (1997) 429.